International Journal of Fatigue 65 (2014) 58–63

Contents lists available at ScienceDirect

International Journal of Fatigue

journal homepage: www.elsevier.com/locate/ijfatigue

Experimental characterization of short crack nucleation and growth during cycling in lean duplex stainless steels

R. Strubbia [a,*], S. Hereñú [a], A. Giertler [b], I. Alvarez-Armas [a], U. Krupp [b]

[a] Instituto de Física Rosario – CONICET, Universidad Nacional de Rosario, Argentina
[b] Faculty of Engineering and Computer Science, University of Applied Sciences Osnabrück, Germany

ARTICLE INFO

Article history:
Received 23 January 2013
Received in revised form 20 August 2013
Accepted 28 August 2013
Available online 5 September 2013

Keywords:
Duplex stainless steel
Fatigue
Crack nucleation
Microstructure
EBSD

ABSTRACT

Considering that many applications of Lean Duplex Stainless Steels (LDSSs) involve cyclic loading, the aim of this paper is to study short crack initiation and growth during low (LCF) and high cycle fatigue (HCF) in AL 2003 (UNS S32003). Electron Backscattered Diffraction (EBSD) analysis of plastically active grains allows to determinate the slip systems and their associated Schmid factor (SF). Additionally, the dislocation structure developed during cycling is observed by transmission electron microscopy (TEM). Whereas in HCF cracks nucleate at grains boundaries, during LCF cracks nucleate along intrusion/extrusions in ferritic grains and as they reach austenitic grains grow along active slip systems or by double slip system. Moreover, phase boundaries and grain boundaries act as effective barrier against crack propagation.

1. Introduction

Duplex stainless steels (DSS) are two-phase alloys with approximately equal proportions of ferrite (α) and austenite phases (γ). The duplex microstructure combines properties of both phases that may even be enhanced in the mixture; the ferrite provides high strength and resistance to stress corrosion cracking, while the austenite contributes to good ductility and general corrosion resistance [1,2]. Recently, many companies have tried to reduce the cost of duplex stainless steels replacing more expensive elements, like Ni, by other lower cost elements, giving rise to a low-alloyed grade of DSS named Lean DSS. To maintain the typical microstructural balance of DSS, the reduction in Ni content is compensated by an increasing amount of Mn and N elements.

LDSSs are being used in many industrial applications subject to cyclic loading [3]. Fatigue damage generally initiates at plastic strain concentration sites. These are the result of different stages during fatigue, which starts with the evolution of dislocations structure and the consequent localization of the strain and the final nucleation and propagation of cracks [4]. Particularly, short crack behavior is influenced not only by loading conditions but also by microstructural features including chemical composition, volume fraction of phases, phase distribution, grain size and heat treatment [5]. Some researchers [6–9] have studied short crack nucleation in standard DSS during fatigue. However, in low-alloyed duplex stainless steels there is scarce information correlating the dislocation structure, the evolution of the surface damage and short crack nucleation on low-alloyed duplex stainless steels [10]. Therefore, the aim of this work is to study microstructural short cracks nucleation and propagation during LCF as well as short cracks nucleation HCF in a LDSS and the correlation with the dislocation structure developed in both fatigue regimes.

2. Material and experimental procedure

2.1. Material

The investigated material was the AL 2003 (UNS S32003) LDSS. This steel was received in longitudinally welded stainless steel pipe. The manufacturing process of the pipes includes a hot rolled stage and a subsequent welding of the tube. A thermal treatment at 1050 °C followed by a rapid water quench was finally carried out to the tube. The chemical composition of the present LDSS in weight percent is: C:0.021; Cr:22; Ni:3.8; Mo:1.8; Mn:1.73; Si:0.22; P:0.024; N:0.18; Fe: balance. The yield stress of the LDSS AL 2003 is 579 MPa. From slabs taken parallel to the axis of the pipe, flat specimens for low and high cycle fatigue were prepared. Fig. 1a shows the geometry of the specimen used for fatigue tests. An optical micrograph from the as-received LDSS is observed in Fig. 1b. The microstructure morphology consists mainly of a lamellar structure of bright austenite islands embedded in a grey etched ferrite matrix. This steel presents approximately the same volume fraction of austenite and ferrite. The EBSD technique was used for

* Corresponding author.
E-mail address: strubbia@ifir-conicet.gov.ar (R. Strubbia).

0142-1123/$ - see front matter © 2013 Elsevier Ltd. All rights reserved.
http://dx.doi.org/10.1016/j.ijfatigue.2013.08.023

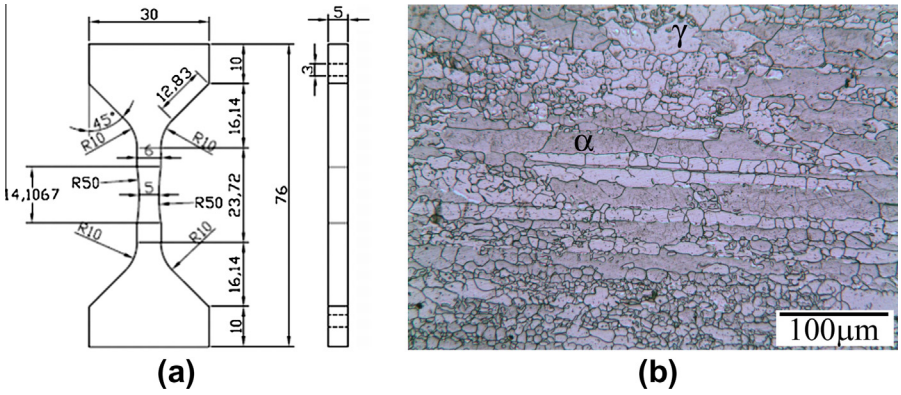

Fig. 1. (a) Specimen geometry and (b) microstructure of AL 2003.

grain size determination. The average grain size and their standard deviations are 7 ± 4 μm for the ferritic phase and 4 ± 2 μm for the austenite. Vickers hardness was measured in both phases; the values obtained were 310 ± 10 for ferrite and 320 ± 10 for austenite.

2.2. Specimen preparation

Specimens for mechanical tests were initially ground and polished with sequentially finer grits paper and finally were electrolitically polished; using A2 supplied by Struers as electrolyte. This surface preparation allows the observation of the structure during tests and the acquisition of good quality electron back-scattered diffraction patterns (EBSD).

2.3. Mechanical tests

In order to observe the damage evolution during LCF tests, a central sector of the specimens was selected. Surface damage observations of this zone were performed by in situ microscopy before and during the LCF test using an optical system composed of a CCD camera JAI mod. CM-140MCL with a 50× objective, focal length of 13 mm, depth of field of ±1 μm and a 12× ultra zoom device mounted on the fatigue test machine. LCF tests were conducted at room temperature under fully reversed plastic strain control, at a constant total strain rate $\dot{\varepsilon} = 2 \times 10^{-3}\ s^{-1}$, with a plastic strain range $\Delta\varepsilon_p = 0.2\%$. The LCF test with these conditions was repeated five times so as to discern the occurrence of the initial slip lines with the surface relief in each phase and to calculate theirs corresponding standard deviations.

Besides, push–pull HCF tests were carried out in servo-hydraulic testing system at room temperature under stress control with stress amplitude of $\sigma = 425$ MPa, stress ratio $R = -1$ and frequency $f = 10$ Hz. In situ observation of specimens during HCF was not possible because the optical system mounted on the HCF testing machine does not allow discerning the small grains of the AL 2003. This optical system is composed of a long-distance QUESTAR optical microscope coupled to a digital camera.

In order to compare the strain rates in LCF and HCF tests, the total strain rate of HCF tests was estimated. This quantity was approximated as the ratio between twice the total strain range measured at midlife to fracture (Nf /2) and the frequency, resulting that $\dot{\varepsilon}$ is of the order of $1 \times 10^{-1}\ s^{-1}$.

2.4. Slip systems determination

After LCF and HCF tests a Scanning Electron Microscope (SEM) equipped with EBSD detector was used. EBSD measurements provide the Euler angles $(\varphi_1, \Phi, \varphi_2)$ that characterize the three-dimensional orientation of the grains. These data enable to determine the slip systems, their SF and their angles relative to the tensile axis. On the other hand, the angles between the surface slip markings and the loading axis were measured. The comparison of these angles with the calculated ones permits to identify the activate slip systems and theirs corresponding SFs.

2.5. TEM observation

In order to analyze the dislocation structure after fatigue, thin foils were prepared from discs cut parallel to the tensile axis of the specimen using a double-jet electropolisher. The dislocation structures of the as-received material and of the specimens cycled up to failure were observed by TEM operating at 100 kV.

3. Results and discussion

Fig. 2 shows the dislocation structure in the as-received condition in both phases of AL 2003. It is important to remark that after the thermomechanical manufacturing process, considerable dislocation density remains in the bulk.

The optical in situ observations during LCF reveals that the first deformation lines appear in the ferrite phase after 100 ± 50 cycles (Fig. 3a) while in the austenitic phase they appear after 300 ± 100 cycles (Fig. 3b). As cycling proceeds the surface damage evolution is mainly concentrated in the ferrite (Fig. 3c). According to a previous study in this steel [10], some of the slip lines in ferrite evolve to extrusions at the surface where short cracks finally nucleate. The preceding fatigue damage evolution is corroborated in the present work. Moreover, the surface damage observation has also enabled to note that the slip markings have different morphology in each phase. While in the austenite phase the slip bands are straight, in ferritic grains slip lines are wavy. This wavier feature of the ferrite phase is attributed to the high capacity of cross-slip developed by b.c.c structures that allow the activation of several slip systems.

An initiated crack within the ferritic phase can present two alternative crack growing mechanism as it reaches austenitic neighbouring grains (Fig. 4): grows along a favourable slip plane with high SF (stage I), or alternating between two slip systems (stage II). This last growing mechanism has already been reported by others authors [11,12]. Additionally, these authors propose a useful method to calculate the plane of the crack in stage II. Applying this procedure to the present steel, it is found that some cracks grow by double slip on lattice planes of {1 1 0} type (Fig. 4). It is important to remark that independently of the growing mechanism (stage I or II), cracks grow approximately perpendicular to the specimen axis.

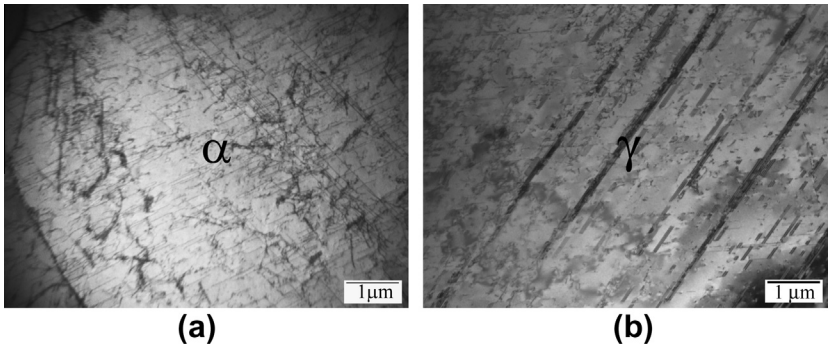

Fig. 2. Dislocation structure of AL 2003 in the as-received condition (a) ferrite and (b) austenite.

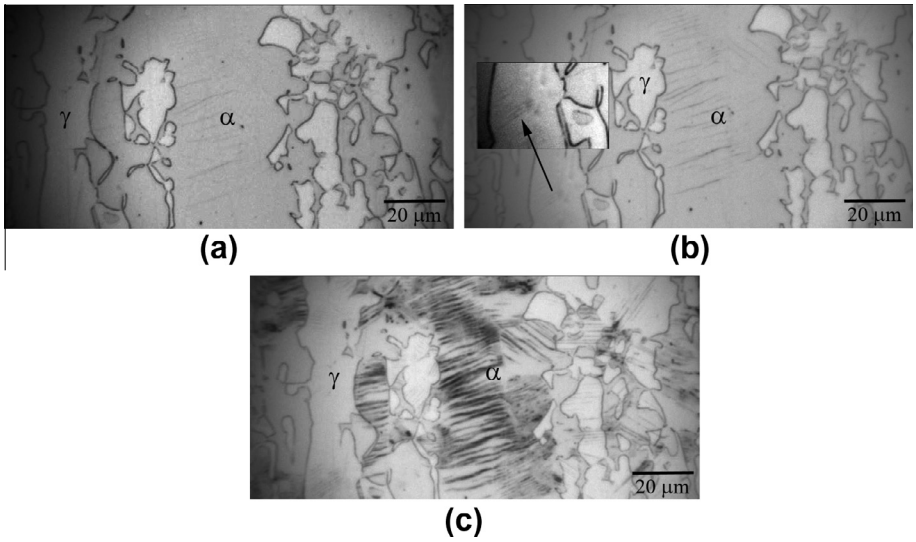

Fig. 3. Slip markings at the surface of LCF specimens after: (a) 100 cycles (b) 300 cycles and (c) 15900 cycles.

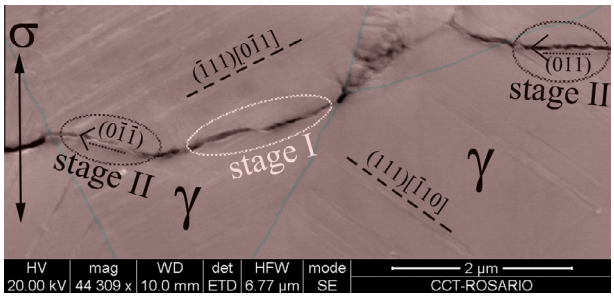

Fig. 4. SEM image superimposed to an EBSD phase map of a LCF specimen showing crack growth mechanisms; stage I and stage II.

Fig. 5 shows the path of a crack after LCF test. As it can be seen in this figure, as well as reported [13,14] in standard DSSs, the microcracks growth in the present material follows an exponential law. Moreover, it seems that the growth rate of microcracks is affected by crystallographic barriers (Fig. 5). In fact, phase boundaries and grain boundaries are effective barrier against crack propagation.

The dislocation structures observed in LCF specimens are characterized by bundles of dislocations in the ferrite phase (Fig. 6a) and by a planar array of dislocations with stacking faults in the austenite phase (Fig. 6b). It is important to remark that ferrite develops a higher dislocation density than austenite during fatigue. Therefore, microcracks nucleation in ferrite during LCF can be rationalized by the larger plastic activity found in this phase.

During HCF the in situ observation of specimens was not possible, so in this case the surface damage in fractured specimens was analyzed. SEM and EBSD measurements reveal that most of the cracks nucleate at grain boundaries, Fig. 7.

TEM observations of HCF specimens show that ferrite phase exhibits a microstructure similar to that observed in the as-received condition (Fig. 8a) whereas the austenite phase presents pile-ups on one, two or three active slip systems (Fig. 8b). As others authors [9,15] have already found in DSS when pile-ups in the austenite are arrested at a grain boundary a zone of high localized stresses is produced generating a high dislocation density (Fig. 9).

In both fatigue regimens, the dislocation structure and crack nucleation sites depend on the plastic deformation sustained by each constituent phase. The mechanical behavior of ferrite phase depends strongly on temperature and strain rates. At low temperature ferrite exhibits asymmetries in tension/compression related to the flow stress and to the active slip plane. These properties are basically a consequence of the extended core structure of the screw dislocation. Glide of a screw dislocation occurs by thermally activated formation of kink pairs. Consequently, the mobility of screw dislocations strongly decreases at temperatures below a transition temperature T_0 (T_0 is between 0.1 and 0.2 Tm, Tm: melting temperature). This temperature, which separates both regimens, is shifted to markedly higher temperature at higher

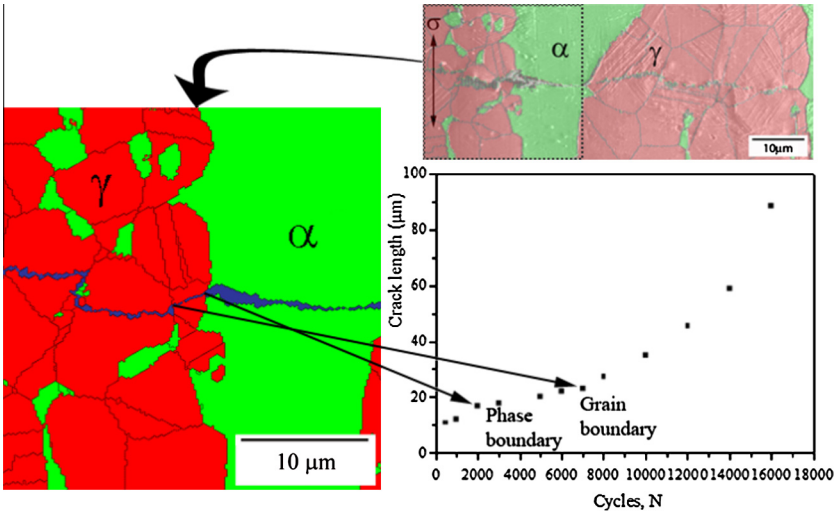

Fig. 5. Superposition of SEM image and EBSD phase map showing the crack path after LCF test and the crack length vs. number of cycles.

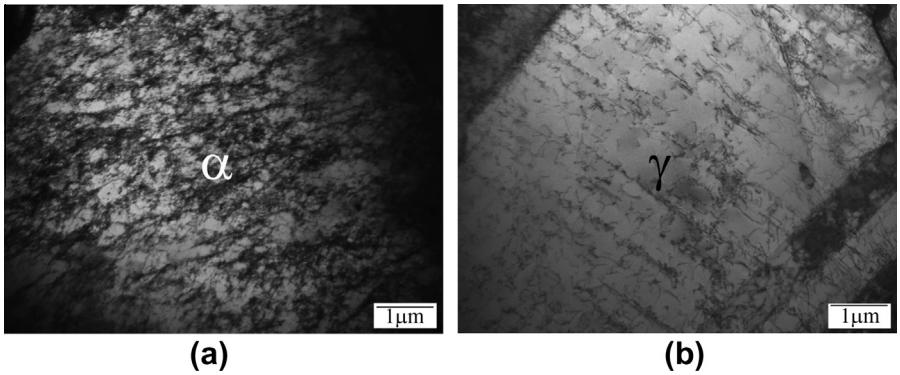

Fig. 6. Dislocation structure in LCF specimens at failure (a) ferrite and (b) austenite.

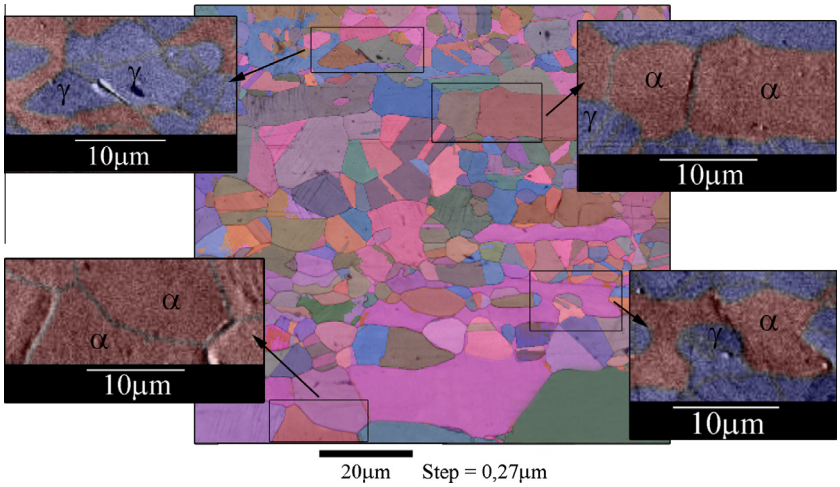

Fig. 7. SEM image and EBSD map showing cracks nucleation in grain boundaries in HCF specimens.

strain rates [16]. Mughrabi [16] has mentioned that at moderate $\dot{\varepsilon}$ ($\leqslant 10^{-4}\ s^{-1}$) the transition temperature lies around the room temperature in the case of α–Fe.

During LCF test, $\dot{\varepsilon}$ (=$2 \times 10^{-3}\ s^{-1}$) was slow enough to consider that T_0 is not so far to room temperature. So, edge and screw dislocations have enough mobility in both phases. On the other hand, the addition of nitrogen to DSS is well known to be responsible for a hardness increase as well as a more planar dislocation glide in the austenite [17–23]. This type of slip character is observed in the austenitic phase of AL 2003 (Fig. 2a). Regarding the structure developed for a planar slip alloys, dislocation motion is restricted to its corresponding slip plane due to the reduce ability of screw

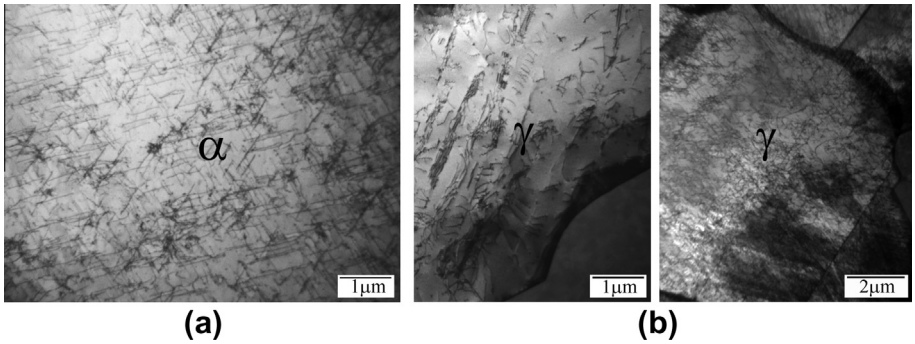

Fig. 8. Dislocation microstructure in HCF specimens fatigued up to failure (a) ferrite (b) austenite.

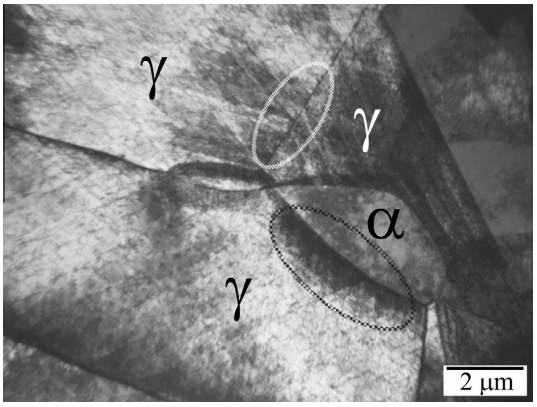

Fig. 9. Zones of high stresses localized in grains boundaries observed in HCF specimens fatigued up to failure.

dislocations to cross slip. So in this case, it is easier for the ferrite phase to accommodate most of the deformation (Fig. 3). These highly strained ferritic grains give way to the formation of extrusions that provoke the appearance of short cracks.

On the other hand, during HCF the strain rate ($\approx 1 \times 10^{-1}$ s^{-1}) was high enough to consider room temperature well below T_0 and thus, screw dislocations will have limited mobility in the ferrite phase. In the studied LDSS crack initiation at α–α boundaries could be attributed to asymmetric slip of screw dislocations, which led to shape changes in neighbouring ferritic grains. Due to the restricted movement of screw dislocations in the ferrite phase, the austenite must bear most of the plastic deformation. Moreover, as the pile-ups in the austenite impinge a grain boundary produce a zone of high stress concentration there (Fig. 9). The fact that the pile-ups are not able to surpass the grains boundaries could explain the microcracks nucleation at γ–γ and α–γ boundaries in HCF regime.

In both fatigue regimens the analysis of activated slip systems reveals that in the austenite grains most of the observed traces correspond to slip systems with SF higher than 0.4, consistent with the results reported by Villechaise et al. [24] in 316L austenitic stainless steel. The determination of the active slip systems in the ferrite is very difficult because each slip trace could be associated with more than one slip system. Nevertheless, through a detailed analysis it is found that some activated slip systems in the ferritic grains present SF below 0.4. This fact agrees with the results reported by others authors in DSS [25–27] and in aged DSS [28]. As proposed by Gironès et al.[28], although the SF is a decisive parameter for the development of plastic activity in the austenite grains, in the ferrite grains other parameters such as strong slip activity in the neighbouring grains must be considered to define the activation of their slip systems.

4. Conclusions

During LCF the plastic deformation is mainly sustained by the ferrite phase. This could explain the cracks nucleation along intrusion/extrusions in this phase. When the cracks reach the austenite neighbouring grain, it grows by combined slip on adjacent slip planes or along favourable slip planes. Moreover, phase boundaries and grain boundaries act as effective barrier against crack propagation.

During HCF cracks nucleate at grains boundaries. Cracks nucleation at α–α boundaries could be attributed to asymmetric slip of screw dislocations. On the other hand, stress localization at grain boundaries could cause crack nucleation at γ–γ and α–γ boundaries.

In both fatigue regimes the active slip systems in austenitic grains have SF higher than 0.4. Conversely, some active slip systems observed in ferrite have SF lower than 0.4.

Acknowledgements

This work was supported by Agencia Nacional para la Promoción de la Ciencia, Técnica and Consejo Nacional de Investigaciones Cientícas y Técnicas (CONICET) and by the cooperation program DAAD/MinCyT between Germany and Argentina.

References

[1] Gysel W, Dybowski G, Wojtas HJ, Schenk R. Proc. Duplex Stainless Steels'86; 1986. p. 98–108.
[2] H. D. Solomon and T.M. Devine, Duplex Stainless Steel–A tale of two phase, Proc. Duplex Stainless Steels '82. (1982) 693–756.
[3] E. Alfonsson, Lean duplex–the first decade of service experience, in 8th Duplex Stainless Steels conference. 2010.
[4] Polák J, Kruml T, Obrtlík K, Man J, Petrenec M. Short crack growth in polycrystalline materials. Proc Eng 2010;2(1):883–92.
[5] Miller KJ., The behavior of short fatigue cracks and their initiation, Fatigue Fract Eng Mater Struct. 10 1(1987) 75–91.
[6] Alvarez-Armas I, Marinelli M, Malarria J, Degallaix S, Armas A. Microstructure associated with crack initiation during low-cycle fatigue in a low nitrogen duplex stainless steel. Int J Fatigue 2007;29(4):758–64.
[7] Bartali AE, Alvarez-Armas I, Marinelli MC, Moscato MG, Signorelli JW. K-S relationship identification technique by EBSD. Key Eng Mater 2011;465:415–8.
[8] Stolarz J, Foct J. Specific features of two phase alloys response to cyclic deformation. Mater Sci Eng, A 2001;319–321:501–5.
[9] Alvarez-Armas I, Krupp U, Balbi M, Hereñú S, Marinelli MC, Knobbe H. Growth of short cracks during low and high cycle fatigue in a duplex stainless steel. Int J Fatigue 2012;41:95–100.
[10] Strubbia R, Hereñú S, Marinelli MC, Alvarez-Armas I. Short crack nucleation and growth in lean duplex stainless steels fatigued at room temperature. Int J Fatigue 2012;41:90–4.
[11] Richter R, Tirschler W, Blochwitz C. In-situ scanning electron microscopy of fatigue crack behaviour in ductile materials. Mater Sci Eng, A 2001;313(1–2):237–43.
[12] Düber O, Kunkler B, Krupp U, Christ H, Fritzen C. Experimental characterization and two-dimensional simulation of short-crack propagation in an austenitic–ferritic duplex steel. Int J Fatigue 2006;28(9):983–92.

[13] Polak J, Zezulka P. Short crack growth and fatigue life in austenitic-ferritic duplex stainless steel. Fatigue Fract Eng Mater Struct 2005;28(10):923–35.
[14] Balbi M, Avalos M, El Bartali A, Alvarez-Armas I. Microcrack growth and fatigue behavior of a duplex stainless steel. Int J Fatigue 2009;31(11–12):2006–13.
[15] Marinelli MC, Krupp U, Kübbeler M, Hereñú S, Alvarez-Armas I. The Effect of the embrittlement on the fatigue limit and crack propagation in a duplex stainless steel during high cycle fatigue. Engineering Fracture Mechanics 2013.
[16] Mughrabi H. Dislocations in fatigue. Dislocations Prop Real Mater 1985;323:244–61.
[17] Akdut N, Keichel J, Foct J. The influence of nitrogen and orientation on the rolling deformation mechanisms of austenitic single crystals. Steel Res 1997;68(11):495–500.
[18] Wahlberg G, Rolander U, Andren HO. Interaction between nitrogen and substitutional elements in the austenitic phase of duplex austenitic–ferritic stainless steels. In: Foct J, Hendry A, editors, HNS '88, Proceedings of the 1st international conference on high nitrogen steels, Lille (France), London, The Institute of Metals; 1989. p. 163.
[19] Grujicic M, Nilsson JO, Owen WS, Thorwaldsson T. Basic deformation mechanisms in nitrogen strengthened stable austenitic stainless steels. In: Foct J, Hendry A, editors, HNS '88, Proceedings of the 1st International conference on high nitrogen steels, Lille (France), London, The Institute of Metals; 1989. p. 151.
[20] Sassen J, Garrat-Reed AJ, Owen WS. Electron microscopy of austenitic Fe–Ni–Cr alloys containing nitrogen. In: Foct J, Hendry A, editors. HNS '88. Proceedings of the 1st international conference on high nitrogen steels, Lille (France), London, The Institute of Metals; 1989. p. 159.
[21] Li Y, Laird C. Cyclic response and dislocation structures of AISI 316L stainless steel. Part 1: Single crystals fatigued at intermediate strain amplitude. Mater Sci Eng 1994;A186:65–86.
[22] Li Y, Laird C. Cyclic response and dislocation structures of AISI 316L stainless steel. Part 2: Polycrystals fatigued at intermediate strain amplitude. Mater Sci Eng 1994;A186:87–103.
[23] Foct J, Akdut N. Cleavage-like fracture of austenite in duplex stainless steel. Scr Met Mater 1993;29:153–8.
[24] Villechaise P, Sabatier L, Girard JC. On slip band features and crack initiation in fatigued 316L austenitic stainless steel: Part 1: Analysis by electron back-scattered diffraction and atomic force microscopy. Mater Sci Eng A 2002;323(1–2):377–85.
[25] Vogt JB, Salazar D, Proriol Serre I. Partition of cyclic plasticity in the 25Cr–7Ni–0.25N duplex stainless steel investigated by atomic force mycroscopy. In: Alvarez-Armas I, Degallaix-Moreuil S, editors, Duplex stainless steels, 2009. p. 275–302 [chapter 8].
[26] Marinelli MC, El Bartali A, Signorelli JW, Evrard P, Aubin V, Alvarez-Armas I, et al. Activated slip systems and microcrack path in LCF of a duplex stainless steel. Mater Sci Eng, A 2009;509(1–2):81–8.
[27] El Bartali A, Aubin V, Sabatier L, Villechaise P, Degallaixmoreuil S. Identification and analysis of slip systems activated during low-cycle fatigue in a duplex stainless steel. Scripta Mater 2008;59(12):1231–4.
[28] Gironès P, Villechaise A, Mateo M, Anglada, Méndez J. EBSD studies on the influence of texture on the surface damage mechanisms developed in cyclically loaded aged duplex stainless steels. Mater Sci Eng, A 2004;387–389:516–21.